Mismatch Repair by Efficient Nick-Directed, and Less Efficient Mismatch-Specific, Mechanisms in Homologous Recombination Intermediates in Chinese Hamster Ovary Cells

Elizabeth M. Miller, Heather L. Hough, Jennifer W. Cho and Jac A. Nickoloff

Department of Cancer Biology, Harvard University School of Public Health, Boston, Massachusetts 02115

Manuscript received March 25, 1997
Accepted for publication June 20, 1997

ABSTRACT

Repair of single-base mismatches formed in recombination intermediates *in vivo* was investigated in Chinese hamster ovary cells. Extrachromosomal recombination was stimulated by double-strand breaks (DSBs) introduced into regions of shared homology in pairs of plasmid substrates heteroallelic at 11 phenotypically silent mutations. Recombination was expected to occur primarily by single-strand annealing, yielding predicted heteroduplex DNA (hDNA) regions with three to nine mismatches. Product spectra were consistent with hDNA only occurring between DSBs. Nicks were predicted on opposite strands flanking hDNA at positions corresponding to original DSB sites. Most products had continuous marker patterns, and observed conversion gradients closely matched predicted gradients for repair initiated at nicks, consistent with an efficient nick-directed, excision-based mismatch repair system. Discontinuous patterns, seen in ~10% of products, and deviations from predicted gradients provided evidence for less efficient mismatch-specific repair, including G-A → G-C specific repair that may reflect processing by a homologue of *Escherichia coli* MutY. Mismatch repair was >80% efficient, which is higher than seen previously with covalently closed, artificial hDNA substrates. Products were found in which all mismatches were repaired in a single tract initiated from one or the other nick. We also observed products resulting from two tracts of intermediate length initiated from two nicks.

DNA mismatches arise during DNA replication and recombination, and from spontaneous or genotoxin-induced chemical modification of DNA. During recombination, heterologous point mutations, insertions, and deletions can produce heteroduplex DNA (hDNA) with mismatched bases and loops. Mismatch repair has recently gained increased attention with the finding that defects in mismatch repair systems predispose to cancer. Deficiencies in mismatch repair systems in prokaryotes and yeast lead to genome instability and mutator phenotypes (LEVINSON and GUTMAN 1987; STRAND *et al.* 1993), and these phenomena are also observed in some human cancers (AALTONEN *et al.* 1993; BOYER *et al.* 1995), including human hereditary nonpolyposis colon cancer (HNPCC). HNPCC was shown to result from a defect in mismatch repair (reviewed in KOLODNER 1995), and other tumor types were subsequently found to harbor mutations in HNPCC-associated loci (BOYER *et al.* 1995).

Mismatch repair in *Escherichia coli* can be divided into two categories (for review see MODRICH 1991). The general pathway can repair all types of single- and multiple-base mismatches and is mediated by *mutHLS*, although certain mismatches (*e.g.*, C-C) are not repaired unless repair is initiated at a second, linked mismatch. This pathway depends on mismatch recognition by MutS, which then complexes with MutL. MutH endonuclease nicks the unmethylated DNA strand in hemimethylated DNA immediately following replication to initiate excision/resynthesis of that strand to repair the mismatch. These repair tracts can be longer than a kb, and MutH was shown to be dispensable in nicked substrates (LAHUE *et al.* 1989). In contrast, MutT and MutY are involved in short tract G-T → G-C and G-A → G-C repair, respectively. Mismatch repair systems in eukaryotes are less well characterized, although both *Saccharomyces cerevisiae* and mammalian cells have protein homologues to MutL and MutS suggesting conservation of long tract repair. In human cell extracts, G-T mismatches were preferentially repaired to G-C (WIEBAUER and JIRICNY 1989), indicating at least one short patch system exists in mammals, and genetic evidence is also consistent with the presence of these systems in higher eukaryotes (HEYWOOD and BURKE 1990; STEEG *et al.* 1990; CARROLL *et al.* 1994).

The *in vitro* and *in vivo* correction of all possible single-base mismatches has been reported for yeast and mammalian cells (BISHOP and KOLODNER 1986; BROWN and JIRICNY 1988; HOLMES *et al.* 1990; VARLET *et al.* 1990; THOMAS *et al.* 1991; FANG and MODRICH 1993), and differential repair efficiencies and biased repair have been observed. *E. coli* has both strand-dependent (*mutHLS* pathway) and mismatch-dependent (*mutT* and *mutY* pathways) repair biases. Studies in mammalian

Corresponding author: Jac A. Nickoloff, Department of Molecular Genetics and Microbiology, School of Medicine, University of New Mexico, Albuquerque, NM 87131. E-mail: jnickoloff@salud.unm.edu

cells have yielded conflicting results. HARE and TAYLOR (1985) found that methylation status and nicks influenced strand discrimination in African green monkey kidney CV-1 cells, and *in vitro* studies indicated that nicks are strong signals for strand-specific mismatch repair in human cells (HOLMES *et al.* 1990; FANG and MODRICH 1993; UMAR *et al.* 1994). In contrast, HEYWOOD and BURKE (1990) found that nicks did not control strand targeting in monkey COS-7 cells.

We previously described a system for studying mismatch repair in hDNA formed during extrachromosomal recombination in mammalian cells (DENG and NICKOLOFF 1994). A limited study in Chinese hamster ovary (CHO) cells involving two single-base mismatches separated by 2 bp suggested that nicks predicted to be adjacent to hDNA may impose a strand bias on the repair of these mismatches. That study further indicated that the system would allow simple experimental control of the extent of hDNA, and of the types and positions of mismatches formed in recombination intermediates. The present work expands on that previous work in several ways. First, we obtained support for the hypothesis that the hDNA region can be controlled by varying the positions of double-strand breaks (DSBs) in input recombination substrates. Second, the influence of nicks on mismatch repair was assessed in crosses that generated multiple, single-base mismatches at varying distances from predicted nick sites, and our results indicate nick-directed mismatch repair is an efficient repair mode. Third, the closely spaced markers (separated by ~100-bp intervals) provided information about co-mismatch repair, and less efficient, short tract repair of specific types of mismatches. Finally, segregation analysis performed in this study and a separate study (D. G. TAGHIAN and J. A. NICKOLOFF, unpublished results) indicate that CHO cells repair mismatches in recombination intermediates with high efficiency.

MATERIALS AND METHODS

Plasmid DNA constructions: Plasmids were constructed using standard procedures (SAMBROOK *et al.* 1989), and during cloning plasmid DNA was prepared as described previously (DENG and NICKOLOFF 1992). For transfection into mammalian cells, plasmids were prepared by acidic-phenol extraction, as described by WANG and ROSSMAN (1994). This method yields largely supercoiled plasmid preparations, thus limiting the amount of nonspecific nicks in recombination substrates. Four plasmids were used as recombination substrates (Figure 1A). A *neo* allele (*neo11;* Figure 2) containing 11 mutations was created from pneo (NICKOLOFF and REYNOLDS 1990), a pUC19 derivative with a 1.4-kbp *Sal*I-linked *Hin*dIII/*Sma*I fragment of pSV2neo (SOUTHERN and BERG 1982). The 11 mutations each created new restriction sites (RFLPs) and were introduced during four rounds of unique-site elimination mutagenesis (DENG and NICKOLOFF 1992). All RFLPs were phenotypically silent, consisting of single base substitutions up- or downstream of the *neo* coding sequence, or at third positions in *neo* codons (Table 1). Plasmid pSV2neoX(B) was constructed from pSV2neo by insertion of a 10-bp *Xho*I linker (5′dCCCTCGAGGG3′) into the *Bss*HII site of *neo*. The 11 RFLPs were transferred from pneo11 to pSV2neoX(B) by a domain replacement procedure (RAY *et al.* 1994), which also eliminated the *Xho*I mutation, creating pSV2neo11. The *Xho*I mutation was then recreated as described above to produce pSV2neo11X(B). The RFLPs were also transferred to pneoAn (NICKOLOFF and REYNOLDS 1990) creating pneoAn11. The identities of mutations were confirmed by sequence analysis and/or restriction mapping. A control plasmid was made by deleting a 703-bp *Bam*HI/*Eco*RI fragment (containing the SV40 late region) from pSV2neoX(B), creating pSV2neoX(B)-late. A second control plasmid with the 11 RFLPs, pSV2neo11-late, was similarly constructed from pSV2neo11. These control plasmids have the same gross structure as that predicted for rescued recombinant products and were used in RFLP analysis of recombinant products (see below).

TABLE 1

Silent mutations in *neo11* and mismatches produced when *neo11* anneals with wild-type *neo*

Mutation[a]	Change[b]	Enzyme[c]	Mismatches[d]: Mutant base donated by	
			pSV2neo	pneoAn
H251	G → C	*Hin*dIII	C-C	G-G
B349	G → C	*Bam*HI	C-C	G-G
A430	A → C	*Apa*I	C-T	A-G
A523	C → A	*Apa*LI	A-G	C-T
P685	C → A	*Pst*I	A-G	C-T
B733	T → G	*Bam*HI	G-A	T-C
N871	C → G	*Nru*I	G-G	C-C
N928	C → A	*Nsi*I	A-G	C-T
P1030	C → A	*Pml*I	A-G	C-T
X1135	T → A	*Xba*I	A-A	T-T
H1239	G → C	*Hin*dIII	C-C	G-G

[a] Numbers in mutation names indicate position in *neo*.
[b] Wild-type base in coding strand listed first, mutant base second.
[c] Enzyme recognizing RFLP mutation.
[d] Coding strand bases are listed first.

Cell culture and recombination assays: CHO K1c cells were cultured in αMEM supplemented with 10% v/v fetal bovine serum (Intergen), 25 mM HEPES buffer, 100 units/ml penicillin G, and 100 μg/ml streptomycin sulfate. Cells were grown at 37° in 5% CO_2 and 90% humidity. Under these conditions the doubling time was ~16 h. For transformations, plasmid substrates were linearized at appropriate restriction sites (Figure 2) and purified by passage through Sepharose CL-6B (NICKOLOFF 1994). Subconfluent CHO cell populations were trypsinized, suspended in complete medium, then collected by centrifugation. The cell pellet was washed with 40 ml of calcium/magnesium-free PBS (CMF-PBS), counted, and centrifuged again. The pellet was then resuspended in an appropriate volume of CMF-PBS to obtain a cell density of 5.3×10^6 cells/ml. Cell suspension (0.75 ml) was mixed with 50 μl CMF-PBS containing 0.02–5 μg of each linearized recombination substrate. A 300 V/960 μF shock was delivered to the cell/DNA suspension with a Bio-Rad Gene Pulser. Shocked cells were transferred to 250 ml of prewarmed, complete medium. Plating efficiency was determined by plating dilutions of electroporated cells into nonselective medium; the remainder of the cell suspension was distributed among 24-well plates, at 1.5 ml per well. The plates were incubated at 37° for 24 h before addition of G418 (1250 μg/ml, 65% active, GIBCO). Plating efficiency averaged 80–90% that of untreated cells.

Analysis of recombinant products: After 12 days of growth

in selective medium, wells containing colonies were trypsinized and the cell suspension redistributed in the same well in selective medium to expand cell populations to confluence. Genomic DNA was then prepared by a modification of a nonorganic method described by GRIMBERG *et al.* (1989). Briefly, cells were rinsed with PBS, then lysed by incubating 4–6 hr in 0.4 ml of 20 mM Tris-HCl (pH 7.6), 100 mM NaCl, 10 mM EDTA, 0.5% SDS, and 0.1 mg/ml proteinase K (Sigma) at 37°. Solutions were transferred to a 1.5 ml tube; 150 μl of 5 M NaCl were added and the contents mixed by inversion. The tubes were then centrifuged at 2000 × *g* for 15 min; supernatants were transferred to a clean 1.5 ml tube. Tubes were filled with 100% ethanol and mixed by inversion to precipitate the DNA. The DNA was centrifuged at 2000 × *g* for 5 min. Pellets were air dried, suspended in 200 μl TE containing 1 mg/ml RNase, and incubated at 37° for 1 hr. Twenty microliters of 3 M sodium acetate (pH 7.0) were added. The tubes were filled with 100% ethanol and mixed by slow inversion, and the DNA was pelleted at 2000 × *g* for 5 min, rinsed with 80% ethanol, air dried for 10–15 min, and then resuspended in 50 μl TE.

Recombinant products were transferred from CHO cells to *E. coli* for analysis ("rescued") as follows. Integrated recombinant plasmids were released from genomic DNA by digestion with *Eco*RI and circularized with T4 DNA ligase at low concentration (<50 μg/ml), which minimizes concatemer formation. In some cases, ligated DNA was treated with *Xho*I, which linearizes nonrecombinant plasmids [pSV2neoX(B) or pSV2neo11X(B)] that may have also integrated. Because linear DNA transforms *E. coli* less efficiently than circular DNA (CONLEY and SAUNDERS 1984), *Xho*I digestion was used to improved rescue efficiencies in some crosses. Ligated DNA was concentrated to 10 μl and electroporated into *E. coli* HB101 as described (MILLER and NICKOLOFF 1995). Plasmid DNA from ampicillin- and kanamycin-resistant (amp^r, kan^r) colonies was prepared. Generally, >75% of rescued plasmids had the structure expected for products arising from a nonconservative exchange between pSV2neo and pneoAn derivatives. Other products were not unexpected since integrated, nonrecombinant pneoAn derivatives will also yield amp^r, kan^r bacterial transformants upon rescue, and unwanted genomic DNA fragments may ligate to rescued plasmids. These incorrect plasmids were easily identified by *Stu*I/*Eco*RI digestions as they produce a different restriction pattern than the control plasmid, pSV2neoX(B)-late. Because the only *Stu*I site in recombination substrates occurs in the SV40 promoter of pSV2neo derivatives, this enzyme digestion provides a means to distinguish amp^r, kan^r recombinant products that carry the SV40 promoter from pneoAn, which lacks this promoter. *Stu*I/*Eco*RI digestion also distinguishes nonrecombinant pSV2neo derivatives (which yield 2.7- and 2.9-kb fragments) from recombinants (2.2 and 2.7 kb). RFLP sites were scored in recombinants by using mapping strategies analogous to those described previously (SWEETSER *et al.* 1994). To assure product independence, plasmid DNA was prepared and analyzed from only one amp^r, kan^r colony per G418-resistant ($G418^r$) CHO colony, except during segregation analysis (described below). Results are reported as percentage conversion for each RFLP, indicating a change in the sequence connected to the SV40 promoter, the "recipient" allele; in crosses 1A, 2A, and 3A, which used pSV2neo11X(B), conversion indicates RFLP loss, and in crosses 1B, 2B and 3B, which used pSV2neoX(B), conversion indicates RFLP gain. For each cross, mismatch repair tract spectra were generated by scoring all markers in 20–39 independent recombinant products. Statistical analysis was performed using Fisher exact tests.

Segregation analysis: To measure mismatch repair efficiency, products were analyzed as described above except that sets of at least six plasmids were rescued and analyzed from each independent CHO colony. For this analysis, only 20 ng of each substrate was used, which reduces the chance of wells containing more than one colony and of transfectants carrying more than one integrated recombinant *neo*. These were identified by Southern hybridization of genomic DNA digested with *Stu*I (one site in recombinants, diagnostic for tandem integrated molecules) or with *Bst*XI (no site in recombinants, diagnostic for nontandem, multiple copies of integrated molecules), using ^{32}P-labeled *neo* as a probe (DENG and NICKOLOFF 1994). When all rescued products of a set yielded the same pattern for a particular marker, this was taken as an indication of repair at that marker (confidence limit ~0.97); if two patterns were obtained, this indicated mismatch segregation at the first round of replication following integration, which produces a mixed or "sectored" CHO colony.

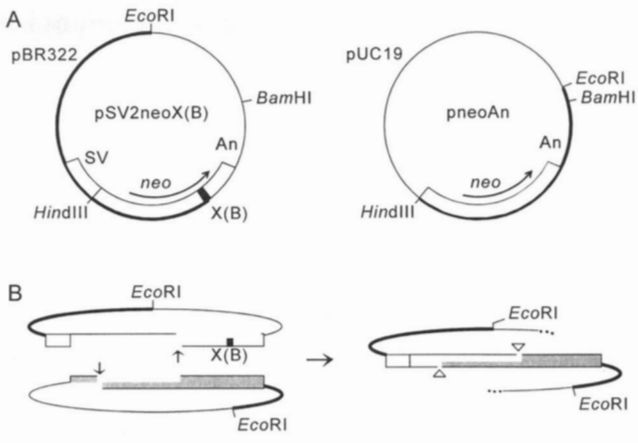

FIGURE 1.—Recombination substrates. (A) In pSV2neo derivatives, *neo* is driven by the SV40 promoter and inactivated the X(B) frameshift mutation (black bar). *neo* in pneoAn derivatives has a wild-type coding sequence but lacks a promoter. Derivatives with *neo11* have these same structures but contain 11 silent RFLPs (not shown). *Eco*RI sites are used in plasmid rescue; heavy lines indicate regions isolated in rescued recombinants. (B) Extrachromosomal recombination as predicted by the SSA model and rescue strategy. Shading indicates *neo11* sequences. DSBs (arrows) are processed to single-stranded regions, exposing complementary strands that anneal to produce a nonconservative crossover product with hDNA flanked by single-strand breaks in opposite strands (triangles) corresponding to DSB sites. Recombinant molecules are rescued from genomic DNA by digesting with *Eco*RI, recircularizing with DNA ligase, and transforming *E. coli*.

RESULTS

Experimental design: We employed an extrachromosomal recombination system to study mismatch repair in intermediates produced *in vivo*. DSBs in plasmid substrates are predicted to stimulate recombination through a single-strand annealing (SSA) pathway first proposed by STERNBERG and colleagues (LIN *et al.* 1984, 1990a,b). In this model, strand annealing forms hDNA flanked by nicks in opposite strands corresponding to DSB positions, yielding nonconservative crossover products (Figure 1B). Two studies with related systems in mouse and Xenopus cells provided some evidence for hDNA formation, but the majority of the data was interpreted in terms of a model that lacked extensive hDNA

(because few markers segregated and few discontinuous tracts were observed), suggesting instead that exchange occurred between two molecules at a discreet point ("simple exchange") (DESAUTELS *et al.* 1990; CARROLL *et al.* 1994). Because these events are nonconservative, such exchange can be thought of as a half-crossover event. However, these results can also be interpreted using an hDNA model if repair is efficient. Current evidence, described in detail in DISCUSSION, favors the hDNA model and the results of the present study are therefore presented in this light. Although there is evidence for alternative extrachromosomal recombination pathways in mammalian cells (YANG and WALDMAN 1992), the great majority of products can be explained by the SSA model. Even when only one plasmid is broken, or neither is broken, essentially all products of such two-plasmid systems can be explained by SSA (J. A. NICKOLOFF and R. J. REYNOLDS, unpublished results). In crosses with circular molecules, it is likely that nicks are introduced into substrates during transfection, and these nicks are acted on by an exonuclease that exposes single strands. All crosses in the present study employed linear plasmids to optimize SSA recombination, because our primary goal was to examine mismatch repair of hDNA formed *in vivo*.

Our previous study using singly marked *neo* alleles (DENG and NICKOLOFF 1994) indicated that this two-plasmid system would allow experimental control of hDNA extent and location (by introducing DSBs at specific sites in *neo*), and of the types of mismatches formed when strand annealing produces a recombination intermediate (by using *neo* heteroalleles with defined markers). To extend this work, we performed crosses predicted to form multiple mismatches. *neo* alleles were constructed with 11 phenotypically silent, single-base RFLP mutations at ~100-bp intervals and used in three pairs of crosses (Figure 2). The silence of the RFLPs was demonstrated by introducing plasmids individually into *E. coli* and CHO cells. pSV2neo11, carrying only silent mutations, conferred kan^r to *E. coli* (data not shown) and G418^r to CHO cells; transfection frequencies were similar with or without silent mutations (Table 2). Thus, there was no selective pressure for or against RFLP markers. Plasmids bearing *neo* with the X(B) frameshift mutation did not yield kan^r *E. coli* transformants or G418^r CHO transfectants (Table 2). pneoAn and pneoAn11 have wild-type *neo* coding capacity and confer kan^r to *E. coli*. Although these plasmids lack a mammalian promoter, they produced G418^r CHO transfectants at low frequencies (~10^{-6}; Table 2) as found previously (DENG and NICKOLOFF 1994). This is at least 30-fold lower than recombination frequencies. These rare colonies most likely reflect integration near an endogenous promoter; they do not interfere with product analysis as they do not yield a rescued plasmid with the appropriate recombinant structure (see MATERIALS AND METHODS).

In this system, recombination occurs between a derivative of pSV2neo in which *neo* driven by the SV40 promoter is inactivated by a frameshift mutation and a second plasmid carrying *neo* with intact coding sequence but lacking a promoter (Figure 1B). DSBs are introduced in the 3′ region of *neo* in pSV2neo derivatives and 5′ region of *neo* in pneoAn or pneoAn11. Recombination is stimulated at least 10-fold less when a DSB is present in only one plasmid, or if DSBs are in the reverse orientation (J. A. NICKOLOFF and R. J. REYNOLDS, unpublished results). Recombinant plasmids were integrated into CHO genomic DNA, conferring G418^r, and were then rescued into *E. coli* for detailed marker analysis as described in MATERIALS AND METHODS. Mismatch repair may occur either before or after integration; if one or more mismatches escape repair, the resulting sectored colony can be identified by segregation analysis.

hDNA formation in a defined region *in vivo*: Three pairs of crosses were performed with DSBs introduced into the *Bgl*II site of pneoAn or pneoAn11, and at three positions in pSV2neo derivatives (Figure 2). Markers outside of the DSBs were predicted to be outside of hDNA and therefore all recombinants from all crosses were expected to retain the marker configuration of the pSV2neo derivative for H251 (the sole marker 5′ of the *Bgl*II site). Thus, recombinants were expected to have H251 in crosses 1A, 2A and 3A, which employed pSV2neo11X(B), but this marker should be absent in the corresponding "B" crosses using pSV2neoX(B). Similarly, all RFLP mutations 3′ of *Msc*I were expected to be absent in products of cross 1A, but present in cross 1B; analogous predictions can be made for markers 3′ of *Rsr*II and *Bst*BI in crosses 2 and 3, respectively. In contrast, markers between the DSBs were predicted to be in hDNA and therefore these markers could be present or absent in recombinant products. The data from these six crosses, summarized in Figures 3–5, are completely consistent with these predictions. Thus, this system allows experimental control over the position and extent of hDNA in recombination intermediates.

An efficient nick-directed mismatch repair mechanism in CHO cells: hDNA was predicted to include three silent markers in crosses 1A and 1B, seven in crosses 2A and 2B, and nine in crosses 3A and 3B. In addition, hDNA in crosses 2 and 3 included the X(B) frameshift mutation and G418^r products are expected only if X(B) is lost or escapes repair. In our previous study, a single marker was located asymmetrically between the DSBs, and repair was biased in a manner consistent with an excision repair process directed from the proximal nick (DENG and NICKOLOFF 1994). If such processing is general and efficient, a gradient of repair is expected when multiple markers are located in hDNA. If repair initiates at either nick with equal probability and extends in either direction with equal efficiency, conversion rates for any marker would be proportional to its position in hDNA relative to nicks ("percent hDNA"). (Marker positions can be considered

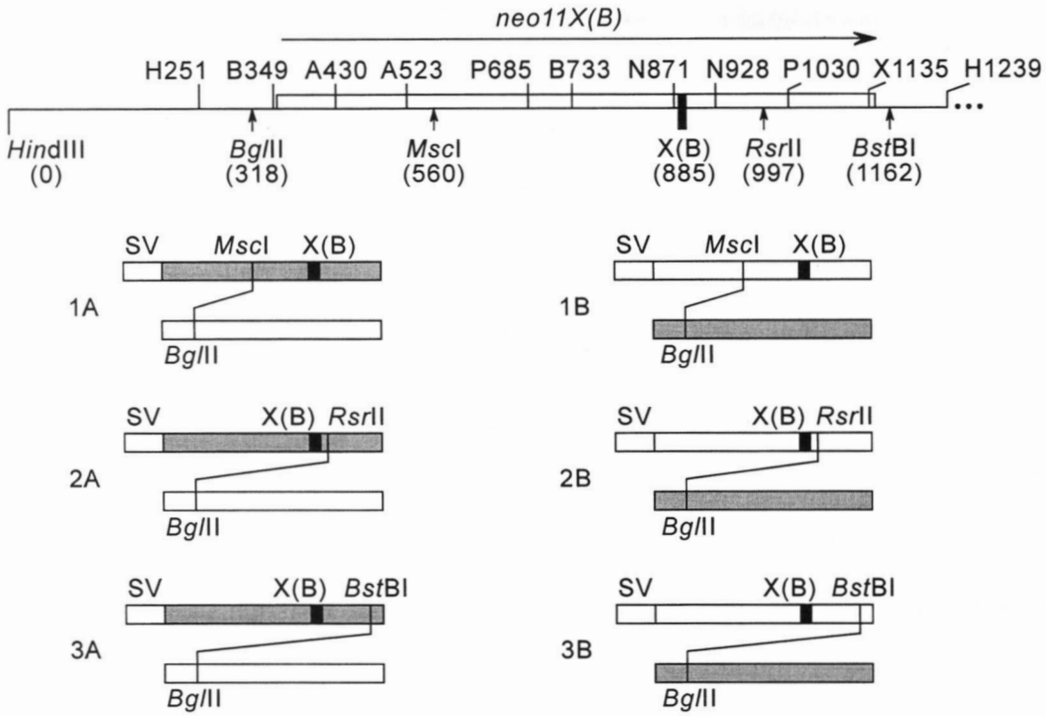

FIGURE 2.—Map of *neo11* and crosses performed. The *neo* coding region is shown by the box. RFLPs are shown above the line, wild-type sites below. Positions are numbered from the *Hin*dIII site upstream of *neo* in pSV2neo. Three sets of crosses are diagrammed below. Crosses differed by the locations of RFLPs (shading) and DSBs (diagonal lines).

relative to 5′ or 3′ nicks, and the same conclusions are reached; here we define percentage hDNA in the 5′ to 3′ direction). For example, in cross 1A, the A523 RFLP is 43 bp from the 3′ nick (corresponding to the *Msc*I cut site), but 201 bp from the 5′ nick (at *Bgl*II), and it is therefore located at a position corresponding to 82% of the total hDNA. If hDNA is processed by efficient nick-directed repair, this marker should be converted more often than retained since the mutant base, which is present in the strand donated by pSV2neo11X(B), should be removed and replaced with the complement of the wild-type base at position 523, donated by pneoAn. The opposite situation holds for B349, which should be retained more often since it is located at 13% of hDNA. The repair tract spectrum shown in Figure 3A is consistent with these expectations, as A523 converted at a rate of 71% and B349 at 21%. A graphical representation of these spectra shows a clear repair gradient, consistent with an efficient nick-directed mismatch process (Figures 3B, 4B and 5B). This gradient is not mismatch specific: cross 1B yields different mismatches at the same positions relative to the nicks as cross 1A (Table 1), yet crosses 1A and 1B have similar gradients (Figure 3B).

TABLE 2

Transfection and recombination frequencies

Expt.	Cross[a]	Plasmid 1	Enzyme	Plasmid 2	Enzyme	Frequency ($\times 10^5$)[b]	n[c]
1	—	pSV2neo	*Eco*RI	—	—	28.6 ± 8.3	3
2	—	pSV2neo11	*Eco*RI	—	—	29.9 ± 8.9	3
3	—	pSV2neoX(B)	*Msc*I	—	—	<0.01	1
4	—	pSV2neo11X(B)	*Msc*I	—	—	<0.03	1
5	—	pneoAn	*Bgl*II	—	—	0.3 ± 0.0	2
6	—	pneoAn11	*Bgl*II	—	—	0.2 ± 0.1	2
7	1A	pSV2neo11X(B)	*Msc*I	pneoAn	*Bgl*II	18.1 ± 1.3	2
8	1B	pSV2neoX(B)	*Msc*I	pneoAn11	*Bgl*II	6.7 ± 2.0	2
9	2A	pSV2neo11X(B)	*Rsr*II	pneoAn	*Bgl*II	18.1	1
10	2B	pSV2neoX(B)	*Rsr*II	pneoAn11	*Bgl*II	13.9	1
11	3A	pSV2neo11X(B)	*Bst*BI	pneoAn	*Bgl*II	19.8	1
12	3B	pSV2neoX(B)	*Bst*BI	pneoAn11	*Bgl*II	11.5	1

Expt., experiment.

[a] Crosses are diagrammed in Figure 2.

[b] Recombination and transfection frequencies were calculated as the ratio of G418^r colonies per cell plated. Values are averages ± SD for experiments repeated three times, averages ± range for experiments repeated twice. From 0.02 to 5 μg of each DNA was used; all frequencies are normalized to 1 μg of DNA.

[c] Number of repetitions.

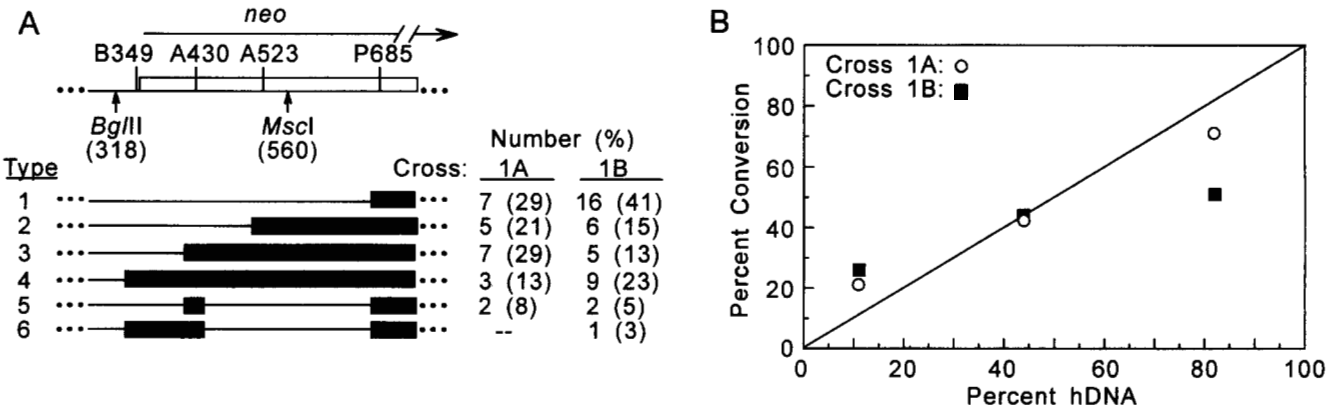

FIGURE 3.—(A) Product spectra for crosses 1A and 1B. A partial map of *neo11* drawn to scale shows the location of RFLPs relative to DSB sites (arrows). Below are listed product types recovered, with bars indicating markers repaired toward the pneoAn derivative sequence ("conversion") and drawn to show maximum tract lengths. Tract types 1–4 are continuous; types 5–6 are discontinuous. All products carried the marker from pSV2neo derivatives upstream of *Bgl*II (H251, not shown), and all markers from pneoAn derivatives downstream of *Msc*I. The number and percentage of each product type are given; — indicates no products recovered. (B) Percentage conversion of individual RFLPs as a function of RFLP position in total predicted hDNA. Diagonal line indicates values predicted if all mismatch repair were nick-directed.

Product spectra for crosses 2A-2B and 3A-3B produce similar repair gradients (Figures 4B and 5B). However, in these cases, the X(B) frameshift mutation is included in hDNA. Since X(B) is absent in G418^r recombinants, markers near X(B) show altered repair patterns. For example, N871 is only 14 bp 5′ of X(B), and corepair of this tightly linked marker leads to high rates of N871 conversion. This was particularly noticeable in crosses 3A and 3B, where N871 converted significantly more often than expected if percentage conversion matched percentage hDNA ($P \leq 0.05$). Nick-directed conversion of X(B) via excision must initiate at the 3′ nick and this would always co-convert markers that occur in hDNA 3′ of X(B). The high conversion rates observed for such 3′ markers (*e.g.*, 100% for all three markers in cross 3A) are consistent with this view.

Some markers displayed conversion rates that differed from rates predicted if repair were proportional to their distances from nicks. In cross 1B, the A523 marker (C-T mismatch) converted significantly less often (51%) than expected (84%; $P < 0.0013$). In contrast, this same marker in the reciprocal cross 1A (occupying the identical position in hDNA but producing an A-G mismatch) converted in 71% of products, which is not significantly different than expected ($P = 0.16$). Although these results would suggest that the low conversion rate of A523 in cross 1B is mismatch-specific, the A523 C-T mismatch converted very near to predicted rates in crosses 2B and 3B, and other C-T mismatches in different crosses were repaired at rates consistent with nick-directed events, such as A430 in cross 2A, and both P685 and B733 in cross 2B. Significant deviations from values expected for nick-directed repair events were seen in cross 3A for P685 and B733 ($P < 0.015$ and $P < 0.03$, respectively), and these deviations were mirrored, though not significantly different from expected values, in cross 2A ($P = 0.11$ and $P = 0.16$, respectively). Although P685 and B733 produce A-G

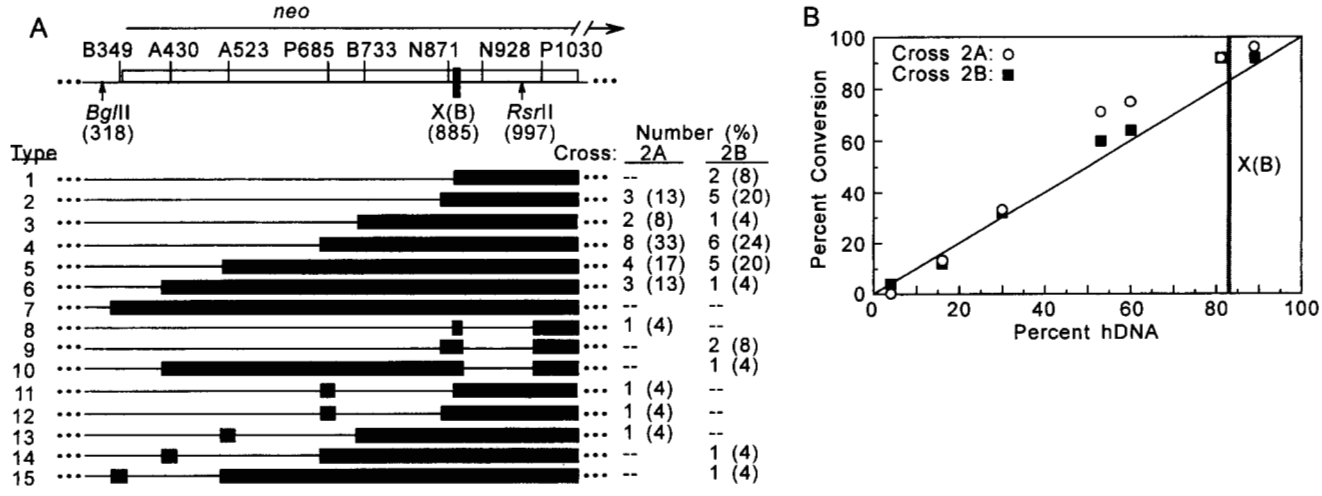

FIGURE 4.—Product spectra for crosses 2A and 2B; see legend to Figure 3 for explanation. In part B, the vertical gray line indicates the position of X(B) in hDNA.

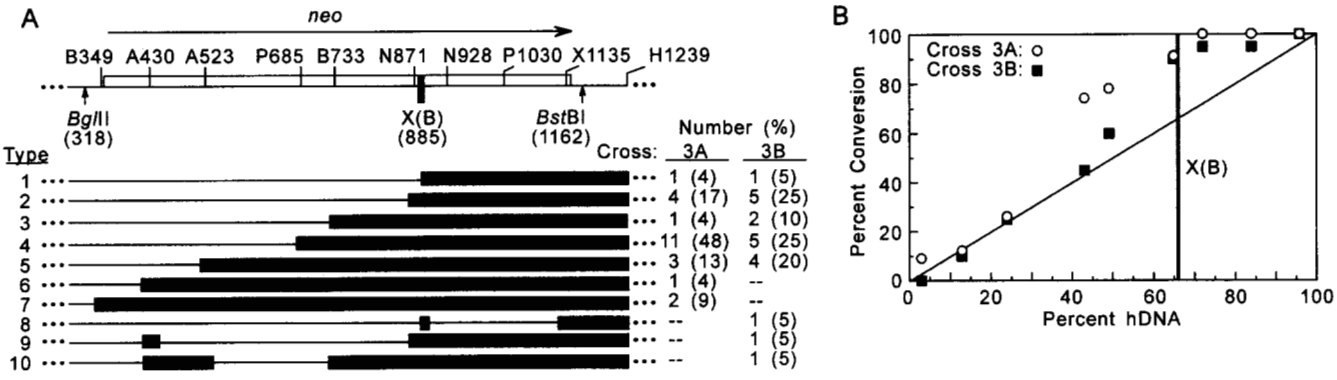

FIGURE 5.—Product spectra for crosses 3A and 3B.

mismatches in crosses 2A and 3A, the observed deviations are due to repair in favor of G for P685 and against G for B733, so these results also do not appear to reflect mismatch-specific repair processing. They may instead reflect corepair effects due to the proximity of these markers to X(B), as discussed above. However, other evidence presented below indicates that there is a degree of specific G-A → G-C repair.

Mismatch repair is efficient: Several lines of evidence argue that hDNA forms in the region defined by the DSBs (see DISCUSSION). Under this assumption, we set out to determine whether tract spectra reflect efficient mismatch repair by performing segregation analysis for crosses 1A and 1B as described in MATERIALS AND METHODS. Repair was assessed at 18 independent mismatches (three markers in hDNA in each of six products), and we observed only three cases in which mismatches escaped repair (83% repair efficiency). Only limited analysis was performed for the present study because a similarly high repair efficiency (94%) was previously determined for 50 independent single-base mismatches in a related cross (D. G. TAGHIAN and J. A. NICKOLOFF, unpublished results). In crosses 1A and 1B, complete repair was observed for the C-C and G-G mismatches, and examples of no repair were seen for both C-T and A-G mismatches (Table 3); these mismatch-specific repair patterns were also seen in the analysis of the other 50 mismatches.

Segregation analysis was not performed for crosses 2 and 3 as these included X(B) in hDNA, and this frameshift mutation could skew the results since only a portion of the possible segregation products would be recovered in media with G418.

Evidence for mismatch-specific repair: Most of the products shown in Figures 3–5 are consistent with long-tract mismatch repair since conversion tracts are continuous (this result is also consistent with simple exchange in intervals, but this view is inconsistent with other data; see DISCUSSION). This result, and the clear conversion gradients shown in Figures 3B, 4B, and 5B, provide strong evidence for an efficient excision-based mismatch repair processing system. However, among the six crosses examined, an average of 11% of tracts were discontinuous (Table 4) and excision repair alone cannot produce such discontinuities. Although they could arise from multiple crossover events, several lines of evidence argue against this view (see DISCUSSION). Instead, it is likely they reflect mismatch-specific repair at single-base mismatches, the X(B) loop mismatch, or both. A total of 15 products had silent markers that were apparently repaired independently of nicks (types 5 and 6 in crosses 1A and 1B; types 11–13 in cross 2A and types 9, 10, 14, and 15 in cross 2B; and types 9 and 10 in cross 3B; Figures 3A, 4A and 5A), although X(B) was also involved in three of these products (types 9 and 10, cross 2B). In 10 of the remaining 12 products the discontinuity involved a single marker. Interestingly, among these 12 products, at least 10 discontinuities involved G-A mismatches and in all 10 cases repair favored the G (Table 4). This bias was independent of whether the G was donated by the pSV2neo or pneoAn derivative.

A second class of discontinuous products (five total) may have arisen from nick-independent repair of the X(B) mismatch (types 8–10 in crosses 2A and 2B, and type 8 in cross 3B; Figures 3A and 4A). In two of these,

TABLE 3

Segregation analysis for crosses 1A and 1B

Event	Cross:	1A	1B	1A	1B	1A	1B	Totals
	Marker:	B349	B349	A430	A430	A523	A523	
	Mismatch[a]:	C-C	G-G	C-T	A-G	A-G	C-T	
Repair toward pSV2neo		2	4	1	2	0	1	10
Repair toward pneoAn		0	0	0	1	2	2	5
Unrepaired		0	0	1	1	0	1	3

[a] First base listed for each mismatch is present in the strand donated by the pSV2neo derivative.

TABLE 4

Percentage and source of discontinuous tracts

Cross	No. of products	No of discontinuous[a]	Mismatch specific repair	
			Silent (G-A)[b]	X(B)
1A	24	2 (8.3)	2 (0)	NA[c]
1B	39	3 (7.7)	3 (3)	NA[c]
2A	24	4 (17)	3 (3)	1
2B	25	5 (20)	3 (2)	2
3A	23	0 (0)	0 (0)	0
3B	20	3 (15)	2 (2)	1
Totals	155	17 (11)	13 (10)	4

[a] Numbers given in parentheses are percentages.

[b] Number of products in which a discontinuity involved one or more silent markers. The number in which a G-A mismatch led to the discontinuity is given in parentheses. In all 10 cases involving a G-A mismatch, the discontinuity resulted from repair favoring G.

[c] Not applicable for crosses 1A and 1B since X(B) was not in hDNA.

X(B) was the sole marker involved in the discontinuity (type 8 in cross 2A, and type 8 in cross 3B). In these two products, and in five others with continuous or discontinuous tracts (type 1 in crosses 2 and 3 and type 11 in cross 3), the X(B) and N871 markers were repaired independently, even though these markers are separated by only 8 bp. The X(B) insertion likely forms a stable palindromic loop mismatch in hDNA and this structure may signal repair that is independent of nicks (discussed below).

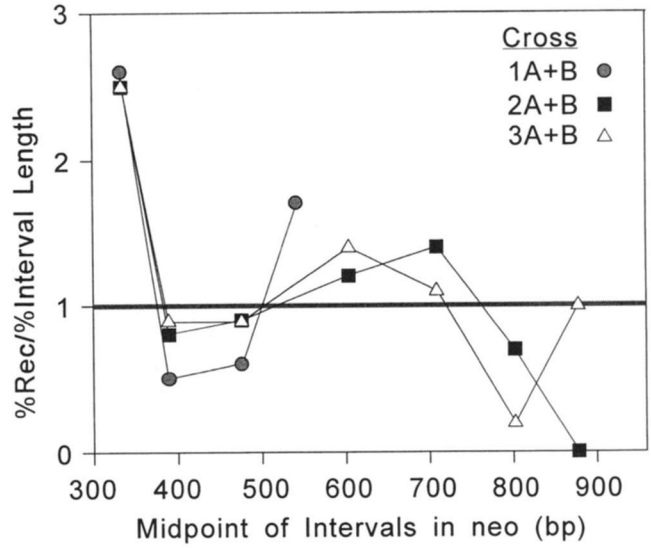

FIGURE 6.—Distribution of recombinants with apparent exchanges in any interval (% Rec) normalized to the length of each interval as a fraction of the total length of predicted hDNA (% interval length) and plotted against the midpoint of each interval in *neo*. This analysis, as described in CARROLL *et al.* (1994), indicates whether particular product types are overrepresented (values > 1) or underrepresented (values < 1) relative to predicted values if exchange occurred in each interval in direct proportion to interval lengths. Values are averages of each pair of A and B crosses; values from individual crosses are similar to these averages (data not shown). Only products with continuous marker patterns are included; thus intervals 3′ of X(B) in crosses 2 and 3 are omitted.

DISCUSSION

Different types of mismatches are repaired with different efficiencies and biases, and bias can result from either mismatch- or strand-specific repair (reviewed in GRILLEY *et al.* 1990). For example, mismatch-specific bias is seen with short tract repair systems (GALLINARI *et al.* 1997), while strand-specific bias can result from nick-directed repair, such as that mediated by *E. coli* MutHLS (MODRICH 1991). Two studies gave conflicting results concerning nick-directed strand bias in monkey cells (HARE and TAYLOR 1985; HEYWOOD and BURKE 1990). We previously obtained evidence for both types of bias in CHO cells. Strand-specific bias was seen with single-base mismatches, and indirect evidence for mismatch-specific bias was found for a 14-bp palindromic loop mismatch (DENG and NICKOLOFF 1994). The present study was undertaken to further investigate the repair of single-base mismatches in CHO cells. In this system, hDNA is putatively formed *in vivo* in recombination intermediates. We therefore first discuss the evidence for hDNA formation by the mechanism shown in Figure 1B.

Recombination via single exchange or mismatch repair in hDNA? Studies in both mammalian cells and Xenopus oocytes support an SSA mechanism for extrachromosomal recombination (CARROLL *et al.* 1994; DENG and NICKOLOFF 1994; LIN *et al.* 1984; LIN *et al.* 1990a; LIN *et al.* 1990b). We show here that multiply marked, nonreplicating recombination substrates generally give products with a single transition point where markers switch from one parental configuration to the other, yielding clear gradients (Figures 3–5). Similar results were obtained with freely replicating substrates in mouse cells by DESAUTELS *et al.* (1990). Because products with a particular transition point arose at frequencies proportional to the length of the interval in which the transition occurred, and "mixed" genotypes were rare, these investigators proposed that most products result from a single crossover and that hDNA was limited (less than a few hundred bp). Our data show a similar proportionality (Figure 6) and rare mixed products, and thus are consistent with the simple exchange model involving minimal hDNA. However, the results are also completely consistent with a different model suggesting that large hDNA regions form, but are subject to efficient, long-tract mismatch repair directed from broken ends. In this view, conversion gradients result from repair tracts initiated from nicks on opposite strands flanking hDNA; proportionality of product frequencies and interval lengths would reflect stochastic termination of long-tract mismatch repair and/or competition between mismatch repair tracts initiating at either end of the hDNA region; and the paucity of

mixed products would reflect highly efficient mismatch repair.

There are five lines of evidence that argue against the simple exchange model. First, discontinuous marker patterns (~11% in all crosses; Table 4) cannot arise by simple exchange but are readily explained by short tract mismatch repair. The products we analyzed cannot result from two exchanges because all products have an SV40 promoter from a pSV2neo derivative linked to the 3′ end of *neo* from pneoAn, and this linkage requires an odd number of interactions. It seems unlikely that discontinuous products would arise from triple exchanges at rates as high as 10–20%. DESAUTELS *et al.* (1990) also found discontinuous patterns in 10% of products, suggested to result from hDNA repair. Second, certain markers convert with bias, including palindromic insertions (DENG and NICKOLOFF 1994; D. G. TAGHIAN and J. A. NICKOLOFF, unpublished results), and those predicted to produce G-A (see below) or G-T mismatches (C. A. BILL and J. A. NICKOLOFF, unpublished results); the latter showed an 87% bias toward G-C, consistent with processing by G-T-specific thymine glycosylase (NEDDERMANN and JIRICNY 1993). Such biases cannot be explained by the simple exchange model, which accounts only for marker intervals, not marker identities. Third, mixed genotypes were found in this study (Table 3) and two other studies (DENG and NICKOLOFF 1994; D. G. TAGHIAN and J. A. NICKOLOFF, unpublished results), providing clear evidence of hDNA. Fourth, transfection of Xenopus cells with artificial hDNA or recombination substrates predicted to produce the same mismatches *in vivo* yielded similar product spectra (CARROLL *et al.* 1994; LEHMAN *et al.* 1994). Finally, compelling evidence for hDNA was obtained in studies with mismatch repair-deficient mutant CHO ("clone B") cells, and near-isogenic wild-type CHOMT$^+$ cells (BRANCH *et al.* 1993). Using a cross involving five RFLP markers in predicted hDNA, wild-type cells yielded no mixed products (of 12 tested) while 53% of 40 products from clone B cells were mixed, and many had multiple markers that escaped repair (D. G. TAGHIAN and J. A. NICKOLOFF, unpublished results). Our previous study of extrachromosomal recombination suggested that hDNA regions could be controlled experimentally by varying positions of DSBs in substrate plasmids (DENG and NICKOLOFF 1994). The current study demonstrates that such control is possible.

Evidence for an efficient nick-directed mismatch repair mechanism: Two prior studies employed multiply marked recombination substrates in mouse or Xenopus cells (CARROLL *et al.* 1994; DESAUTELS *et al.* 1990). If SSA produces hDNA in recombination intermediates, as argued above, then the product spectra in these studies should be analyzed in terms of mismatch repair processing. In both studies, product spectra revealed conversion gradients. Similar gradients were found when multiply mismatched artificial hDNA regions, flanked by nicks, were transfected into Xenopus cells (LEHMAN *et al.* 1994). Thus, despite considerable system differences, product spectra from these studies are quite similar, suggesting a common mechanism. For DSB-induced extrachromosomal recombination, the SSA model predicts nicks on opposite strands flanking hDNA (Figure 1B). Excision repair initiated from a nick will remove markers on that nicked strand. If two nicks are present on opposite strands, repair can initiate from either nick and lead to marker loss or retention. Thus, the direction of repair for a mismatch (conversion *vs.* restoration) will be largely strand-dependent, and determined by which nick is nearest the mismatch; such processing is consistent with the observed conversion gradients. Regardless of whether excision repair tracts initiate at one or both nicks flanking hDNA (discussed further below), the same conversion gradients are predicted. Thus, these gradients suggest that nick-directed repair is an efficient mechanism in CHO cells, as in *E. coli* (MODRICH 1991). Indirect evidence suggests a similarly efficient mechanism exists in yeast, at least for mismatch repair associated with DSB-induced recombination (reviewed in NICKOLOFF and HOEKSTRA 1997).

Mismatch repair efficiency: Segregation analysis indicated that repair is very efficient (at least 80%). However, repair efficiencies did vary, with C-C and G-G repair more efficient than C-T and A-G repair. These relative efficiencies are similar to those obtained with artificial hDNA in covalently closed circular plasmids in monkey and human cells (BROWN and JIRICNY 1988, 1989). However, we found higher overall repair efficiencies, particularly for A-G and C-T mismatches. We observed 81% and 92% repair of A-G and C-T mismatches, respectively, while repair of these mismatches in artificial hDNA were only 39% and 72%. This difference may reflect two factors operating in our system. Nicks may increase repair efficiency by providing an initiation site, and multiple mismatches likely present a stronger signal to the repair machinery than single mismatches. Several lines of evidence support this second point. In yeast, palindromic loop mismatches are poorly repaired unless they are near one or more well-repaired mismatches (PETES *et al.* 1991). In CHO cells, palindromic loop mismatches are well-repaired, and we found a twofold bias in favor of a loop that was equidistant from flanking nicks. However, this bias is eliminated when additional single-base mismatches are included in hybrid DNA, consistent with increased nick-directed repair signaled by single-base mismatches (D. G. TAGHIAN and J. A. NICKOLOFF, unpublished results).

Mismatch-specific repair: We found that ~10% of products had discontinuous conversion patterns, which cannot arise solely by nick-directed repair. Such products could result from either mismatch-specific (short tract) repair or partial repair. Since repair is very efficient, most discontinuities likely arise through mismatch-specific repair. Many of the discontinuities we observed involved G-A mismatches, and the majority of

these apparently arose from biased repair of G-A in favor of G (Table 4). A twofold bias in favor of G among repaired G-A mispairs in artificial hDNA was found previously, although the majority (61%) of these mispairs escaped repair (BROWN and JIRICNY 1988). Biased repair of G-A mismatches in favor of G was first identified in *E. coli* and shown to depend on MutY (reviewed in GALLINARI *et al.* 1997). MutY also processes mispairs arising from oxidative DNA damage, such as 8-oxoguanine-A mispairs (this also results in loss of the A residue). An enzyme with glycosylase/lyase activities, characterized in HeLa cells and calf thymus, is the apparent homologue of MutY and is termed MYH (YEH *et al.* 1991; MCGOLDRICK *et al.* 1995). As this repair activity appears to be widespread in nature, it is likely that a MutY homologue will exist in Chinese hamsters, and that it is responsible for the G-A repair bias we observed.

Because we selected for G418^r recombinants, none contained the inactivating X(B) mutation. In crosses 2 and 3, X(B) is in predicted hDNA, and nick-directed, excision-based repair of X(B) to wild type is limited in two ways. First, X(B) repair cannot initiate at the 5′ nick as this would restore X(B). Second, any markers between the 3′ nick and X(B) will be corepaired (lost) with X(B). We observed five products in which these 3′ markers failed to corepair with X(B) (Figures 4A and 5A). X(B) is a 14-bp palindromic insertion predicted to form a stable stem-loop mismatch. In two studies we obtained genetic (DENG and NICKOLOFF 1994) and physical (D. G. TAGHIAN and J. A. NICKOLOFF, unpublished results) evidence for specific repair of palindromic loop mismatches. Thus, the five products in which X(B) was not repaired from the 3′ nick probably arose from palindrome-specific repair. In summary, the spectra reported here likely reflect the combined activities of efficient, nick-directed repair, and less efficient mismatch-specific repair. Similar conclusions were reached in a study of recombination in Xenopus oocytes (CARROLL *et al.* 1994).

Single or multiple repair tracts? In predicted SSA intermediates, nick-directed repair can occur from one or both nicks. If repair is complete and frequently occurs from only one nick, all markers in hDNA will occur in one or the other parent configuration, such as types 1 and 4 in crosses 1A and 1B (Figure 3A). These two types were overrepresented by about twofold on the basis of product frequency *vs.* interval lengths, yielding a "U" shaped curve in Figure 6. In crosses 2 and 3, repair of X(B) directed from the 5′ nick restores X(B), and therefore it is not surprising that products with apparent exchanges at the 3′ end of *neo* are not overrepresented in these crosses. However, all three sets of crosses showed overrepresentation of products with apparent exchange at the 5′ end of *neo*. These results suggest that a significant fraction of events involve a single repair tract initiating from a nick, and the data from cross 1 further suggests that there is little preference for one end or the other. In Xenopus, single-repair tract products were 10- to 20-fold overrepresented, suggesting greater repair processivity than in CHO cells.

Products with tracts of intermediate length were also relatively common. Although such products could reflect incomplete repair initiated from one end, segregation analysis indicated they usually result from complete repair. This suggests that repair can initiate at both nicks in an intermediate. Such repair could occur sequentially or simultaneously. Sequential repair implies stochastic termination of the initial repair tract. If repair occurs simultaneously, tracts may terminate when repair complexes meet. In this case, if sufficient DNA is not protected from excision (*i.e.*, if the footprint of the repair complex is too small), the intermediate may be destroyed. In any case, the fraction of products with tracts of intermediate length will reflect two factors: repair processivity and competition between two opposing repair complexes.

Can repair also initiate at sites other than nicks predicted to flank hDNA? If, as suggested above, discontinuous tracts generally reflect repair of all mismatches, there are two ways by which these patterns can arise. Using the type 9 product of cross 3B as an example (Figure 5A), we can imagine an initial short tract repair event at A430, followed by 5′ nick-directed repair of B349, A523, P685 and B733, and 3′ nick-directed repair of the remaining markers. Alternatively, initial mismatch-specific restoration of A523 might initiate repair of P685 and B733, followed by 3′ nick-directed repair of all remaining mismatches from X1135 to A430, and 5′ nick-directed repair of B349. In this case, corepair of A523, P685 and B733 might be directed from a nick introduced as a consequence of A523 mismatch-specific repair. There are several other ways to produce these marker patterns, but they are simply variations on these two themes. Additional mismatch repair stimulated by an initial repair event has been proposed to occur in yeast (*e.g.*, BORTS and HABER 1987).

We acknowledge the expert technical assistance provided by DOUG SWEETSER and LAURA GUNN. Helpful comments from COLIN BILL and DANIELLE TAGHIAN are greatly appreciated. This research was supported by grant CA-54079 to J.A.N. from the National Cancer Institute of the National Institutes of Health.

LITERATURE CITED

AALTONEN, L. A., P. PELTOMAKI, F. LEACH, P. SISTONEN, L. PYLKKANEN *et al.*, 1993 Clues to the pathogenesis of familial colorectal cancer. Science **260:** 812–816.

BISHOP, D. K., and R. D. KOLODNER, 1986 Repair of heteroduplex plasmid DNA after transformation into *Saccharomyces cerevisiae.* Mol. Cell. Biol. **6:** 3401–3409.

BORTS, R. H., and J. E. HABER, 1987 Meiotic recombination in yeast: alteration by multiple heterozygosities. Science **237:** 1459–1465.

BOYER, J. C., A. UMAR, J. I. RISINGER, J. R. LIPFORD, M. KANE *et al.*, 1995 Microsatellite instability, mismatch repair deficiency, and genetic defects in human cancer cell lines. Cancer Res. **55:** 6063–6070.

BRANCH, P., G. AQUILINA, M. BIGNAMI and P. KARRAN, 1993 Defective mismatch binding and a mutator phenotype in cells tolerant to DNA damage. Nature **362:** 552–564.

BROWN, T. C., and J. JIRICNY, 1988 Different base/base mispairs are corrected with different efficiencies and specificities in monkey kidney cells. Cell **54:** 705–711.

BROWN, T. C., and J. JIRICNY, 1989 Repair of base-base mismatches in simian and human cells. Genome **31:** 578–583.

CARROLL, D., C. W. LEHMAN, S. JEONG-YU, P. DOHRMANN, R. J. DAWSON *et al.*, 1994 Distribution of exchanges upon homologous recombination of exogenous DNA in *Xenopus laevis* oocytes. Genetics **138:** 445–457.

CONLEY, E. C., and J. R. SAUNDERS, 1984 Recombination-dependent recircularization of linearized pBR322 plasmid DNA following transformation of *Escherichia coli*. Mol. Gen. Genet. **194:** 211–218.

DENG, W. P., and J. A. NICKOLOFF, 1992 Site-directed mutagenesis of virtually any plasmid by eliminating a unique site. Anal. Biochem. **200:** 81–88.

DENG, W. P., and J. A. NICKOLOFF, 1994 Mismatch repair of heteroduplex DNA intermediates of extrachromosomal recombination in mammalian cells. Mol. Cell. Biol. **14:** 400–406.

DESAUTELS, L., S. BROUILLETTE, J. WALLENBURG, A. BELMAAZA, N. GUSEW *et al.*, 1990 Characterization of nonconservative homologous junctions in mammalian cells. Mol. Cell. Biol. **10:** 6613–6618.

FANG, W-H., and P. MODRICH, 1993 Human strand-specific mismatch repair occurs by a bidirectional mechanism similar to that of the bacterial reaction. J. Biol. Chem. **268:** 11838–11844.

GALLINARI, P., P. NEDDERMANN and J. JIRICNY, 1997 Short patch mismatch repair in mammalian cells, in *DNA Damage and Repair*, edited by J. A. NICKOLOFF and M. F. HOEKSTRA. Humana Press, Totowa, NJ (in press).

GRILLEY, M., J. HOLMES, B. YASHAR and P. MODRICH, 1990 Mechanisms of DNA-mismatch correction. Mutat. Res. **236:** 253–267.

GRIMBERG, J., S. NAWOSCHIK, L. BELLUSCIO, R. MCKEE, A. TURCK *et al.*, 1989 A simple and efficient nonorganic procedure for the isolation of genomic DNA from blood. Nucleic Acids Res., **17:** 8390.

HARE, J. T., and J. H. TAYLOR, 1985 One role for DNA methylation in vertebrate cells is strand discrimination in mismatch repair. Proc. Natl. Acad. Sci. USA **82:** 7350–7354.

HEYWOOD, L. A., and J. F. BURKE, 1990 Repair of single nucleotide DNA mismatches transfected into mammalian cells can occur by short-patch excision. Mutat. Res. **236:** 59–66.

HOLMES, J., JR., S. CLARK and P. MODRICH, 1990 Strand-specific mismatch correction in nuclear extracts of human and Drosophila melanogaster cell lines. Proc. Natl. Acad. Sci. USA **87:** 5837–5841.

KOLODNER, R. D., 1995 Mismatch repair: mechanisms and relationship to cancer susceptibility. Trends Biochem. Sci. **20:** 397–401.

LAHUE, R. S., K. G. AU and P. MODRICH, 1989 DNA mismatch correction in a defined system. Science **245:** 160–164.

LEHMAN, C. W., S. JEONG-YU, J. K. TRAUTMAN and D. CARROLL, 1994 Repair of heteroduplex DNA in *Xenopus laevis* oocytes. Genetics **138:** 459–470.

LEVINSON, G., and G. A. GUTMAN, 1987 High frequencies of short frameshifts in poly-CA/TG tandem repeats borne by bacteriophage M13 in *Escherichia coli*. Nucleic Acids Res. **15:** 5523–5538.

LIN, F.-L., K. SPERLE and N. STERNBERG, 1984 Model for homologous recombination during transfer of DNA into mouse L cells: role for DNA ends in the recombination process. Mol. Cell. Biol. **4:** 1020–1034.

LIN, F.-L., K. SPERLE and N. STERNBERG, 1990a Intermolecular recombination between DNAs introduced into mouse L cells is mediated by a nonconservative pathway that leads to crossover products. Mol. Cell. Biol. **10:** 103–112.

LIN, F.-L., K. SPERLE and N. STERNBERG, 1990b Repair of double-stranded breaks by homologous fragments during transfer of DNA into mouse L cells. Mol. Cell. Biol. **10:** 113–119.

MCGOLDRICK, J. P., Y.-C. YEH, M. SOLOMON, J. M. ESSIGMANN and A.-L. LU, 1995 Characterization of a mammalian homolog of the *Escherichia coli* MutY mismatch repair protein. Mol. Cell. Biol. **15:** 989–996.

MILLER, E. M., and J. A. NICKOLOFF, 1995 *Escherichia coli* electrotransformation, pp. 105–113 in *Electroporation Protocols for Microorganisms*, edited by J. A. NICKOLOFF. Humana Press, Totowa, NJ.

MODRICH, P., 1991 Mechanisms and biological effects of mismatch repair. Annu. Rev. Genet. **25:** 229–253.

NEDDERMANN, P., and J. JIRICNY, 1993 The purification of a mismatch-specific thymine-DNA glycosylase from HeLa cells. J. Biol. Chem. **268:** 21218–21224.

NICKOLOFF, J. A., 1994 Sepharose spin column chromatography: a fast, nontoxic replacement for phenol:chloroform extraction/ethanol precipitation. Mol. Biotech. **1:** 105–108.

NICKOLOFF, J. A., and M. F. HOEKSTRA, 1997 Double-strand break and recombinational repair in *Saccharomyces cerevisiae*, in *DNA Damage and Repair*, edited by J. A. NICKOLOFF and M. F. HOEKSTRA. Humana Press, Totowa, NJ (in press).

NICKOLOFF, J. A., and R. J. REYNOLDS, 1990 Transcription stimulates homologous recombination in mammalian cells. Mol. Cell. Biol. **10:** 4837–4845.

PETES, T. D., R. E. MALONE and L. S. SYMINGTON, 1991 Recombination in yeast, pp. 407–521 in *The Molecular and Cellular Biology of the Yeast Saccharomyces: Genome Dynamics, Protein Synthesis, and Energetics*, edited by J. R. BROACH, J. R. PRINGLE and E. W. JONES. Cold Spring Harbor Laboratory Press, Cold Spring Harbor, NY.

RAY, F. A., E. M. MILLER and J. A. NICKOLOFF, 1994 Efficient marker rescue and domain replacement without fragment subcloning. Anal. Biochem. **224:** 440–443.

SAMBROOK, J., E. F. FRITSCH and T. MANIATIS, 1989 *Molecular Cloning: A Laboratory Manual*. Cold Spring Harbor Laboratory Press, Cold Spring Harbor, NY.

SOUTHERN, P. J., and P. BERG, 1982 Transformation of mammalian cells to antibiotic resistance with a bacterial gene under control of the SV40 early region promoter. J. Mol. Appl. Genet. **1:** 327–341.

STEEG, C. M., J. ELLIS and A. BERNSTEIN, 1990 Introduction of specific point mutations into RNA polymerase II by gene targeting in mouse embryonic stem cells: evidence for a DNA mismatch repair system. Proc. Natl. Acad. Sci. USA **87:** 4680–4684.

STRAND, M., T. A. PROLLA, R. M. LISKAY and T. D. PETES, 1993 Destabilization of tracts of simple repetitive DNA in yeast by mutations affecting DNA mismatch repair. Nature **365:** 207–208.

SWEETSER, D. B., H. HOUGH, J. F. WHELDEN, M. ARBUCKLE and J. A. NICKOLOFF, 1994 Fine-resolution mapping of spontaneous and double-strand break-induced gene conversion tracts in *Saccharomyces cerevisiae* reveals reversible mitotic conversion polarity. Mol. Cell. Biol. **14:** 3863–3875.

THOMAS, D. C., J. D. ROBERTS and T. A. KUNKEL, 1991 Heteroduplex repair in extracts of human HeLa cells. J. Biol. Chem. **266:** 3744–3751.

UMAR, A., J. C. BOYER and T. A. KUNKEL, 1994 DNA loop repair by human cell extracts. Science **266:** 814–816.

VARLET, I., M. RADMAN and P. BROOKS, 1990 DNA mismatch repair in Xenopus egg extracts: repair efficiency and DNA repair synthesis for all single base-pair mismatches. Proc. Natl. Acad. Sci. USA **87:** 7883–7887.

WANG, Z., and T. G. ROSSMAN, 1994 Large-scale supercoiled plasmid preparation by acidic phenol extraction. Biotechniques **16:** 460–463.

WIEBAUER, K., and J. JIRICNY, 1989 *In vitro* correction of G-T mispairs to G-C pairs in nuclear extracts from human cells. Nature **339:** 234–236.

YANG, D., and A. S. WALDMAN, 1992 An examination of the effects of double-strand breaks on extrachromosomal recombination in mammalian cells. Genetics **132:** 1081–1093.

YEH, Y.-C., H.-F. LIU, C. A. ELLIS and A.-L. LU, 1991 Two nicking enzyme systems specific for mismatch containing DNA in nuclear extracts from human cells. J. Biol. Chem. **266:** 6480–6484.

Communicating editor: S. JINKS-ROBERTSON